Cancer Research

Therapeutic Inhibition of MAP Kinase Interacting Kinase Blocks Eukaryotic Initiation Factor 4E Phosphorylation and Suppresses Outgrowth of Experimental Lung Metastases

Bruce W. Konicek[1], Jennifer R. Stephens[1], Ann M. McNulty[1], Nathaniel Robichaud[2], Robert B. Peery[1], Chad A. Dumstorf[1], Michele S. Dowless[1], Philip W. Iversen[1], Stephen Parsons[1], Karen E. Ellis[1], Denis J. McCann[1], Jerry Pelletier[2], Luc Furic[2], Jonathan M. Yingling[1], Louis F. Stancato[1], Nahum Sonenberg[2], and Jeremy R. Graff[1]

Abstract

Activation of the translation initiation factor 4E (eIF4E) promotes malignant transformation and metastasis. Signaling through the AKT-mTOR pathway activates eIF4E by phosphorylating the inhibitory 4E binding proteins (4E-BP). This liberates eIF4E and allows binding to eIF4G. eIF4E can then be phosphorylated at serine 209 by the MAPK-interacting kinases (Mnk), which also interact with eIF4G. Although dispensable for normal development, Mnk function and eIF4E phosphorylation promote cellular proliferation and survival and are critical for malignant transformation. Accordingly, Mnk inhibition may serve as an attractive cancer therapy. We now report the identification of a potent, selective and orally bioavailable Mnk inhibitor that effectively blocks 4E phosphorylation both *in vitro* and *in vivo*. In cultured cancer cell lines, Mnk inhibitor treatment induces apoptosis and suppresses proliferation and soft agar colonization. Importantly, a single, orally administered dose of this Mnk inhibitor substantially suppresses eIF4E phosphorylation for at least 4 hours in human xenograft tumor tissue and mouse liver tissue. Moreover, oral dosing with the Mnk inhibitor significantly suppresses outgrowth of experimental B16 melanoma pulmonary metastases as well as growth of subcutaneous HCT116 colon carcinoma xenograft tumors, without affecting body weight. These findings offer the first description of a novel, orally bioavailable MNK inhibitor and the first preclinical proof-of-concept that MNK inhibition may provide a tractable cancer therapeutic approach. *Cancer Res; 71(5); 1849–57. ©2011 AACR.*

Introduction

The translation initiation factor 4E (eIF4E) binds the 5′ m^7GpppN cap structure (where N is any nucleotide) of mRNAs, delivering these mRNAs to the eIF4F complex. This complex, comprised of eIF4E, the ATP-dependent RNA helicase, eIF4A, and the scaffolding protein eIF4G, then scans through and unwinds the 5′untranslated region of the mRNA to reveal the initiation codon and enable translation (1, 2). eIF4F complex assembly is dependent upon eIF4E availability. Under stress conditions such as serum starvation and amino acid depletion, the 4E-binding proteins (4E-BP1, 2, 3) are hypo-phosphorylated and bound to eIF4E, precluding binding of eIF4E to eIF4G. Activation of the AKT-mTOR pathway triggers 4E-BP phosphorylation, liberating eIF4E to engage eIF4G, thereby promoting eIF4F complex assembly (3). Within the eIF4F complex, eIF4E is specifically phosphorylated at serine 209 by the MAPK-interacting kinases (Mnk), which are also bound to eIF4G (4–6). Mnk1 is responsible for inducible phosphorylation of eIF4E, whereas Mnk2 activity is constitutive (7). Both eIF4F complex assembly and the subsequent phosphorylation of eIF4E by Mnks appear to play critical roles in malignant transformation (8–10).

Increased eIF4E function selectively enhances the translation of mRNAs with long, highly-structured 5′ untranslated regions (UTR), as these mRNAs require increased eIF4F complex activity for ribosome loading (1, 2). eIF4E also promotes the nucleocytoplasmic transport of select mRNAs like cyclin D1 (11). eIF4E-regulated mRNAs generally encode proteins involved in key aspects of malignancy including proteins involved in cell growth (cyclin D1, c-myc), angiogenesis (VEGF, FGF-2), invasion (MMP-9, heparanase), and survival (survivin, BCL-2; refs. 1, 12). By selectively upregulating translation of these malignancy-related mRNAs, eIF4E overexpression transforms cells, enabling tumor formation (13) and even metastasis (14). In transgenic mice, ectopic eIF4E expression increases the

Authors' Affiliations: [1]Lilly Research Laboratories, Eli Lilly and Company, Indianapolis, Indiana; and [2]Goodman Cancer Centre and Department of Biochemistry, McGill University, Montreal, Quebec, Canada

Corresponding Author: Jeremy R. Graff, Senior Research Advisor, Cancer Cell Biology and Patient Tailoring, Eli Lilly and Company, Indianapolis, IN 46285. Phone: 317-277-0220; Fax: 317-277-3652; E-mail: graff_jeremy@lilly.com

doi: 10.1158/0008-5472.CAN-10-3298

incidence of multiple cancers, including lymphomas, lung adenocarcinomas, angiosarcomas, and hepatomas (15) and accelerates lymphomagenesis in the *Eμ-myc* mouse lymphoma model (16). In this model, eIF4E phosphorylation by Mnk is critical as mutation of eIF4E at serine 209 or mutational inactivation of Mnk blocks lymphomagenesis (8). Similarly, in *PTEN*-null mouse lymphoma and prostate cancer models, engineered genetic disruption of eIF4E phosphorylation abrogates tumor development (9, 10). In cultured cancer cells, eIF4E phosphorylation has also been shown to be critical for proliferation and survival (17, 18). Importantly, though critical for malignant transformation (8–10), Mnk function and eIF4E phosphorylation are dispensable for normal development (19).

In a wide variety of primary human cancer tissues, eIF4E activation has been linked to disease progression. In ovarian, breast, lung, and prostate cancers, 4E-BP hyperphosphorylation, which increases eIF4E availability, is dramatically increased and related to reduced patient survival (20–23). Overexpression of eIF4E has also been routinely linked to decreased survival in patients with advanced cancers, including head and neck, breast, prostate, lung and hematologic malignancies (1, 12, 22–24). Likewise, more recent work has revealed that eIF4E phosphorylation is specifically increased in advanced malignancies (9, 23–24, Carter JH and colleagues unpublished results).

Collectively, these data implicate enhanced eIF4E function in malignancy and suggest that targeting eIF4E may provide an attractive approach for cancer therapy. Indeed, several inhibitors of eIF4E function have recently been developed. An eIF4E targeted antisense oligonucleotide (ASO) has advanced through phase 1 clinical study (25). An anti-viral guanosine analogue, Ribavirin, which reportedly suppresses eIF4E binding to the mRNA cap structure (26), has progressed through phase 1 studies in acute myeloid patients (AML) patients (27). An inhibitor of the eIF4E: eIF4G interaction, 4EGI-1, has also recently been developed, providing proof of concept that the eIF4F complex can be effectively disrupted by small molecule inhibitors (28).

Targeting eIF4E phosphorylation through direct inhibition of the Mnk kinases is another attractive approach. As Mnk function and eIF4E phosphorylation are dispensable for normal development (19), pharmacologically inhibiting Mnk may provide an avenue to target tumor cells while sparing normal tissues. To date, there are no known, orally bioavailable, selective inhibitors of Mnk. We now report that the antifungal agent, cercosporamide, is a potent, selective, orally bioavailable Mnk inhibitor. Cercosporamide blocks eIF4E phosphorylation in cultured cancer cells, inducing apoptosis, suppressing proliferation, and reducing soft agar colonization. Cercosporamide also effectively blocks eIF4E phosphorylation within 30 minutes after oral administration in normal mouse tissues and xenografted tumors, reduces tumor growth in HCT116 tumor bearing animals, and suppresses the outgrowth of B16 melanoma lung metastases. Collectively, these data substantiate the notion that blocking Mnk function, and eIF4E phosphorylation, may be an attractive anticancer strategy.

Materials and Methods

Cloning, expression, and purification of Mnk1 protein

Mnk1 was cloned by PCR amplification from human lung cDNA (Clontech) with DNA primer sequences 5′-CGCGGATCCCATATGGTATCTTCTCAAAAGTTGG-3′ and 5′-CGCGGATCCACTTAGTCAGAGTGCTGTGGGCGGGCTC-3′, based on *Mnk1* DNA sequence accession number NM_003684.1 and sequence confirmed. The *Mnk1* gene product was cloned into pFASTBAC HTb containing a C-terminal HIS-tag fusion protein, transformed into E. coli DH10 BAC cells, and transfected into Sf9 cells according to the manufacturer's protocol (Invitrogen). Sf9 cells were infected with the viral supernatant to an MOI of 2.0 and incubated at 28°C for 72 hours. Cells were centrifuged and resuspended in 10 mL lysis buffer containing 50 mmol/L Tris, pH 7.5, 150 mmol/L NaCl, 50 mmol/L NaF, 0.5% NP40, 20 mmol/L β-mercaptoethanol, 10 mmol/L Imidazole, 1 mmol/L PMSF, and 1× EDTA-free complete protease inhibitor pellet (Roche). The lysate was centrifuged at 30,000 × *g* for 30 minutes to remove cell debris, and the supernatant was filtered through a 0.2-μm Nalgene filter cup. Purification of Mnk1 protein was performed using an HR 16/10 column (GE Healthcare) packed with Ni/NTA beads (Qiagen) equilibrated in lysis buffer. Filtered cell lysate was loaded followed by a series of column washes, using lysis buffer according to manufacturer's protocol. Mnk1 protein was eluted with 200 mmol/L Imidazole and analyzed by PAGE. Tryptic Digestion of purified protein was performed and analyzed by matrix assisted laser desorption ionisation time-of-flight mass spectrometry (MALDI-TOF MS) for protein confirmation.

High-throughput screen for Mnk1 inhibition

Individual reactions were performed as follows: 0.25 μg purified Mnk1 protein was incubated for 2 hours at room temperature in the presence of 200 μmol/L optimized internal peptide substrate (RRRLSSLRA) in 20 mmol/L HEPES, pH 7.4, 1 mmol/L $MnCl_2$, 2 mmol/L DTT, 1 μmol/L ATP, 0.005% Triton X-100, and 1 μci/well ^{33}P-ATP. Compounds were tested at 10 μmol/L final concentration. Reactions were terminated using 0.5% phosphoric acid with the entire reaction loaded by Multimek onto filter plates (Millipore) pre-wet with 0.5% phosphoric acid, and incubated for 60 minutes at room temperature. Filter plates were extracted twice in 0.5% phosphoric acid. Microscint was added to each well and read on a scintillation counter. A total of 30,000 compounds were screened, and active compounds were defined as having more than 50% inhibition relative to untreated controls. Compounds with potency less than 5 μmol/L were selected for further testing.

CEREP kinase selectivity panel

Cercosporamide was tested at 3 concentrations (0.2, 2, 20 μmol/L) across a panel of 76 kinases (CEREP, Paris, France). Kinases tested included AKT1, AKT2, AKT3, ALK, ALK4, AurA, BRK, CAMK1delta, CDC2/CDK1, CDC7, CDK2, CDK3, CDK5, CDK6, CDK7, CDK9, CHK1, CHK2, CK2, DDR2, DRAK1, DYRK2, EGFR, EphA5, ERK1, Fer, FGFR1, FGFR2, FGFR3, FGFR4, FLT3, FLT4, GSK3β, HIPK2, IKKα, IKKβ, IRAK1,

IRAK4, JAK1, JAK3, JNK3, KDR, LCK, LIMK1, LRRK2, MAPKAPK5, MET, MKK6, MLK1, MNK2, MST1, mTOR, MUSK, p38α, p70S6K, PAK2, PDGFRβ, PDK1, PIM1, PIM2, PKA, PKCβ2, PLK1, PLK2, Raf1, ROCK2, RSK1, RSK3, SGK1, SIK, SRC, TrkA, TrkB, TTK, Tyk2, and WEE1. Kinases that showed inhibition less than 20 μmol/L were retested in 10 point IC_{50} curves.

Western blot analysis

HCT116 and B16 cells were purchased from ATCC and cultured in the recommended media supplemented with 10% FBS. Cells were plated 1 day prior to treatment. CGP5730 was dosed at 20 μmol/L and cercosporamide was dosed at concentrations ranging from 0.625 to 20 μmol/L and incubated for either 1 or 24 hours at 37°C in 5% CO_2. Protein lysates were harvested in Biosource lysis buffer (Invitrogen) and Western blots were run as described (22) with the following antibodies: p-eIF4E 1:500, Mcl-1 1:500 (Cell Signaling), eIF4E 1:1,000 (BD Biosciences), β-actin 1:10,000 (Sigma), mouse and rabbit horseradish peroxidase (HRP)-conjugated secondary antibodies 1:1,000 (Santa Cruz Biotechnology).

Proliferation and apoptosis assays

Cancer cell lines HCT116 (colon), B16 (melanoma), MJ (CTCL), Farage (non-Hodgkins B-cell lymphoma), Calu6, and H1975 (non–small-cell lung carcinoma) were purchased from ATCC and cultured in supplier's recommended media supplemented with 10% FBS. Cells were plated onto poly-D-lysine–coated 96-well plates (BD Biosciences) 1 day prior to treatment. Cercosporamide was dosed at concentrations ranging from 0.156 μmol/L to 20 μmol/L. For proliferation assays, cells were incubated for 6 days in the presence of cercosporamide at 37°C in 5% CO_2. Cells were then subjected to the CellTiter Aqueous 96 One Solution cell proliferation assay (Promega) and measured on a SpectraMax M5 plate reader (Molecular Devices). Response is represented relative to DMSO controls set at 100%. Apoptosis assays were performed after a 72-hour incubation with cercosporamide using the Cell Death Detection ELISA assay (Roche). Apoptosis induction is represented relative to DMSO-treated controls set at 1.0. Error bars denote SEM.

Soft agar colonization assays

In a 6-well plate, 7,500 filtered B16 cells were added in the presence of 10 μmol/L final cercosporamide and 0.35% low melting point agarose onto a bed of 0.7% low melting point agarose with DMEM media containing 10% final FBS final concentration. Compound and cells were mixed for 30 minutes at 4°C. Plates were incubated at 37°C for 14 days, replacing the media with cercosporamide or DMSO every 2 days. After 14 days, media were removed and colonies visualized after incubation with 0.005% crystal violet solution for 1 hour at 37°C. Colonies were scanned and counted using 10% of the area in the counting grid.

Animal studies

All animal work was performed in an Association for Assessment of Laboratory Animal Care (AALAC)-certified facility and was approved by the Eli Lilly and Company Institutional Animal Care and Use Committee. For target inhibition in xenograft tissues and xenograft growth studies, 5×10^6 HCT116 cells were implanted subcutaneously in female athymic *Nu/Nu* nude mice as described (29). Cercosporamide was formulated for oral delivery (0.2 mL/dose) by dissolving compound in one-half volume 20% captisol dissolved in 25 mmol/L phosphate buffer, pH 8.0, followed by addition of an equal volume of 1 mol/L $NaHCO_3$ and briefly sonicated. Cercosporamide was administered p.o. by gavage to mice once the group mean tumor size reached 250 mm^3. Tumor and liver tissues were collected at the indicated time-points. Tissue lysates were prepared as described (29).

To examine the antitumor growth effects of cercosporamide, HCT116 colon carcinoma xenografts were implanted and measured as described (29). Cercosporamide was administered p.o. daily by gavage once mean tumor volumes reached 150 mm^3 and everyday thereafter for 30 consecutive days. Data shown represent tumor volumes at each measured time-point divided by initial tumor volume for each animal (T_1/T_0). Error bars represent SEM. Tumor volume data were transformed to log scale for statistical analyses. *P* values were generated using repeated measures analysis.

For the B16 melanoma experimental pulmonary metastasis model, 100,000 cells were injected into the tail vein of nude mice 1 day prior treatment. Mice were dosed p.o. by gavage with either 10 mg/kg BID or 20 mg/kg q.d. for 12 consecutive days. Lung tissue was collected and placed in 10% neutral buffered-formalin followed by 70% ethanol storage. Individual lung metastases were counted visually. Cercosporamide treatment groups were graphed relative to vehicle-treated control set at 100%. Error bars represent SEM. *P* values were generated using Student's *t* test.

Results

Identification of Mnk inhibitors by high-throughput screen

CGP57380 was reported to be a selective Mnk inhibitor with an IC_{50} of approximately 1 μmol/L (30). Subsequent studies have revealed that this compound effectively inhibits additional kinases at least as potently as Mnk, including CK1 (31). Moreover, this compound, though cell permeable, has not been widely reported for usage in experimental animal models of cancer.

We therefore sought to identify potent, selective Mnk inhibitors that could effectively block eIF4E phosphorylation in cancer cells and in animal models of cancer. A total of 30,000 compounds were screened for inhibitory activity against Mnk1. Twenty-eight compounds were identified with confirmed 10-point IC_{50} values less than 1.0 μmol/L. The most potent compound of these 28 showed an IC_{50} of 116 nmol/L for Mnk1 and 11 nM for Mnk2 (Table 1). This compound is a known antifungal agent named cercosporamide (Fig. 1; ref. 32). To evaluate the selectivity for Mnks versus other kinases, cercosporamide was evaluated at 0.2, 2, and 20 μmol/L against a panel of 76 other kinases. Any kinases showing evidence for inhibition were further tested using 10 point IC_{50} curves. The

Table 1. Kinases inhibited by cercosporamide with IC_{50} values less than 5 μmol/L

Kinase	IC_{50}, μmol/L
Mnk1	0.116
Mnk2	0.011
Jak3	0.031
ALK4	0.356
GSK 3β	0.516
Pim1	0.732
MST	1.18
CDK2	1.64
SIK	1.75
Pim2	2.21
Aur B	2.52
CHK2	2.71
FGFR3	2.96
Flt4	2.98
CDK9	3.53
KDR	4.10

IC_{50} values for these kinases are shown in Table 1. The inhibitory activity of cercosporamide against these other kinases was limited. Jak3, a kinase expressed almost exclusively in hematopoietic tissues (33), was the only kinase inhibited with an IC_{50} of less than 100 nmol/L. Cercosporamide has also been reported to inhibit *Candida albicans* PKC1 (*ca*PKC1) with a 44 nmol/L IC_{50}. However, cercosporamide did not show appreciable activity against human PKCs (PKCα, β, γ, and ε; ref. 34). Consistent with these published data, our kinase profiling data also show that cercosporamide is inactive versus PKCβ2. Collectively, these data reveal that cercosporamide is a potent Mnk inhibitor, with specificity particularly for Mnk2.

Mnk inhibition in cell culture

Mnk1 and 2 phosphorylate a number of intracellular proteins, most notably eIF4E at serine 209, with Mnk2 activity being constitutive and Mnk1 inducible in most cells (7). To assess the cell-based activity of cercosporamide, we evaluated eIF4E phosphorylation (p-eIF4E) by Western blotting. P-eIF4E was evident in all cancer cells tested including B-cell lymphomas (Farage), cutaneous T-cell lymphomas (MJ), the non–small-cell lung cancers (Calu6 and H1975; data not shown), the B16 mouse melanoma line and the human colorectal cancer cell line HCT116 (Fig. 2). In these cell lines, cercosporamide blocked p-eIF4E serine 209 in a dose-dependent manner starting 1 hour after treatment and lasting through at least 24 hours. Similar activity was evident in Calu 6, H1975, Farage B-cell, and MJ cutaneous T-cell lymphoma cell lines (data not shown). CGP57380 (CGP) dosed at 20 μmolL is included for comparison. Levels of p-Erk and p-p38, which can activate Mnks, were unchanged by cercosporamide treatment at 24 hours indicating that blockade of eIF4E phosphorylation was not the result of inhibition upstream of Mnk (Fig. 2C). Importantly, cercosporamide treatment not only reduced eIF4E phosphorylation but also resulted in reduced expression of the antiapoptotic protein Mcl-1 (Fig. 2D), which was previously reported to be regulated by Mnk activity (8).

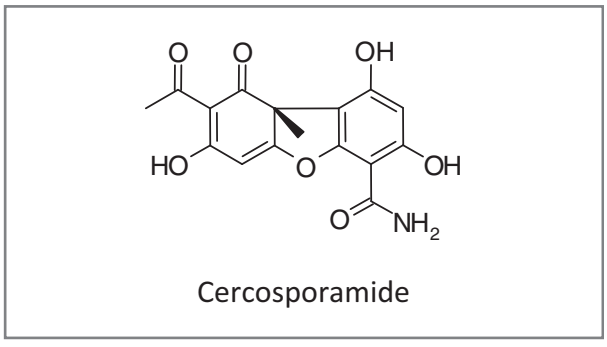

Figure 1. Chemical structure of cercosporamide.

Cercosporamide suppresses cell proliferation, blocks anchorage-independent growth and induces apoptosis

B16 and HCT116 cell lines were treated for 6 days in the presence of cercosporamide (0.6–20 μmol/L) to evaluate whether Mnk inhibition may be antiproliferative *in vitro*. Proliferation was decreased in both cell lines at similar drug concentrations (starting with 2.5 μmol/L; Fig. 3A). We next assessed whether cercosporamide treatment might also block anchorage-independent growth in the B16 melanoma cell line. B16 cells were grown in soft agar for 14 days, with or without 10 μmol/L cercosporamide—a concentration that effectively blocked p-eIF4E levels and suppressed monolayer growth (Fig. 2A). Colony formation was reduced approximately 50% by cercosporamide treatment (Fig. 3B). Because eIF4E phosphorylation has been linked to cell survival (8), we also tested whether Mnk inhibition might be proapoptotic. In both HCT116 and B16 cell lines, apoptosis was induced at cercosporamide concentrations above 2.5 μmol/L (Fig. 3C). To verify that the oligonucleosomal fragmentation data reflected caspase-induced cell death (i.e., apoptosis), we cotreated HCT116 cells with cercosporamide and the caspase inhibitor ZVAD. ZVAD cotreatment completely suppressed cercosporamide-induced oligonucleosomal fragmentation, supporting the notion that cercosporamide elicits a caspase-dependent cell death (apoptosis; Fig. 3D). Collectively, these data show that cercosporamide, at concentrations that effectively inhibit eIF4E phosphorylation (i.e., above 2.5 μmol/L), blocks cellular proliferation and anchorage-independent growth and elicits apoptosis.

Cercosporamide inhibits p-eIF4E in xenografted human tumors and reduces tumor growth

We next examined whether cercosporamide treatment might effectively suppress Mnk activity (i.e., eIF4E phosphorylation) in mice after oral administration. Cercosporamide was delivered p.o. by gavage once at 20 mg/kg in HCT116 tumor-bearing nude mice. Tumor and liver tissues were collected 0.5, 1, 4, and 24 hours after dosing. P-eIF4E levels were reduced in both tumor and liver tissue within 30 minutes of administration and were suppressed in tumor

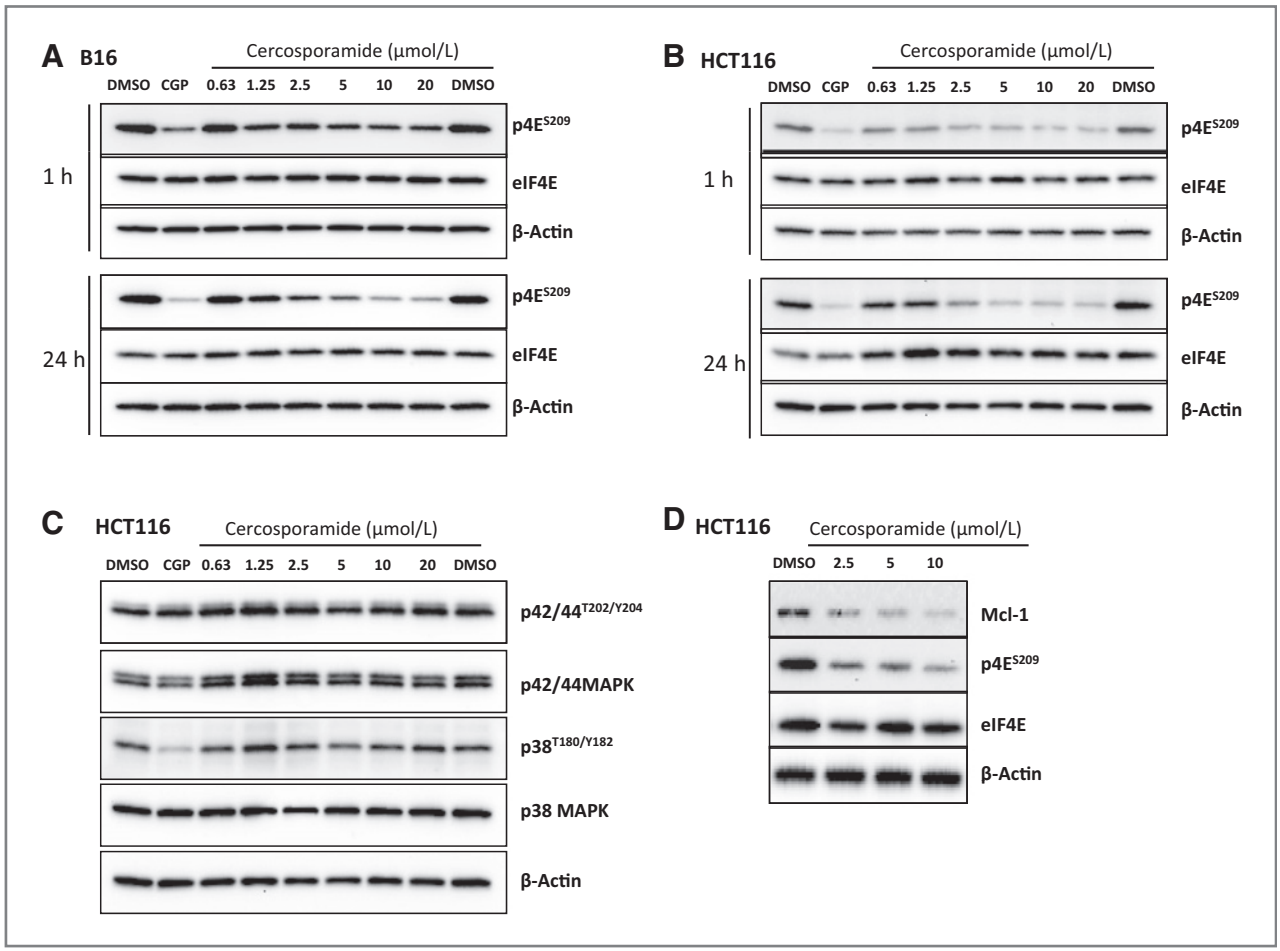

Figure 2. Cercosporamide reduces eIF4E serine 209 phosphorylation levels in cultured cancer cells. Western blot analyses for p-eIF4Eserine 209 in (A) B16 cells or (B) HCT116 cells treated for 1 or 24 hours with cercosporamide (0.625–20 μmol/L), CGP57380 (CGP) at 20 μmol/L, or DMSO as indicated. Companion blots were probed for total eIF4E. C, Western blot analysis for pERK, ERK, p38MAPK, and p-P38MAPK, using HCT116 24-hour lysates from B. D, Western blot analysis for Mcl-1, eIF4E, and $p4E^{ser209}$ in HCT 116 cell lysates treated 24 hours as indicated. All blots were reprobed for β-actin to control for equal protein loading and transfer.

tissue for at least 4 hours, rebounding by 24 hours postdose (Fig. 4A). Moreover, once daily administration of cercosporamide (20 mg/kg) for 30 consecutive days significantly suppressed growth of HCT116 xenograft tumors ($P < 0.05$, repeated measures analyses), without significantly affecting body weight (vehicle control = 21.1 ± 0.6 g; 20 mg/kg cercosporamide = 20.2 ± 0.9 g). These data indicate that oral administration of cercosporamide can effectively inhibit Mnk activity in normal mouse and xenografted human tumor tissues and can significantly suppress xenograft growth.

Cercosporamide suppresses outgrowth of pulmonary metastases

eIF4E overexpression can transform cells (13) and even induce metastases in experimental models (1, 14). Reducing eIF4E expression, even by 50%, suppresses soft agar colonization by more than 90% and significantly reduces the formation and growth of experimental lung metastases (35, 36). We therefore chose to examine whether cercosporamide treatment might suppress experimental lung metastases using the highly pigmented B16 melanoma model. Mice were injected intravenously with 100,000 B16 melanoma cells 1 day prior to treatment to enable these intravenously injected cells to seed within the lungs. The next day, and for 12 consecutive days thereafter, cercosporamide was dosed p.o. by gavage, at either 20 mg/kg once daily or 10 mg/kg twice daily. Mice were sacrificed and lung tissue was collected. Individual lung metastases were counted visually. The numbers of metastases were significantly reduced in both the 10 mg/kg ($P = 0.03$) and 20 mg/kg treatment ($P = 0.02$) groups relative to vehicle controls. Importantly, mice treated with 10 mg/kg twice daily or 20 mg/kg once daily showed only marginal body weight changes (10 mg/kg = 23.4 ± 0.5 g, 20 mg/kg = 25.2 ± 0.4 g) compared with vehicle control (25.6 ± 0.7 g). These data demonstrate that cercosporamide treatment can effectively limit outgrowth of B16 melanoma metastases.

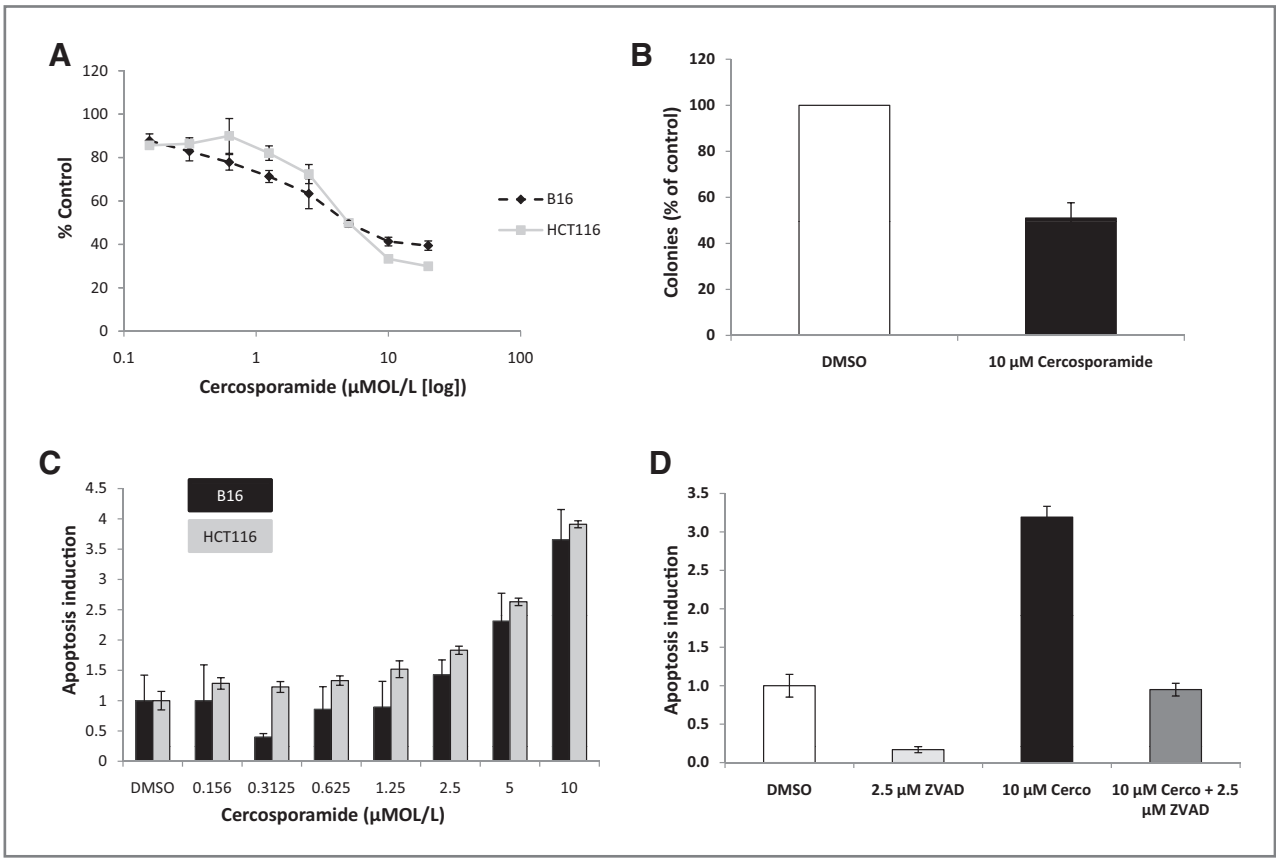

Figure 3. Cercosporamide reduces cell proliferation, inhibits anchorage-independent growth, and induces apoptosis. A, Cellular proliferation was evaluated for HCT116 and B16 cells treated with cercosporamide (0.156–20 μmol/L) over a 6-day time-course. Data are shown relative to DMSO controls set at 100% ± SEM. B, soft agar colony formation by B16 melanoma cells was assessed after 14 days with and without 10 μmol/L cercosporamide. Colonies were visualized by crystal violet stain. Data represent the mean ± SEM from 3 separate experiments graphed as percent relative to vehicle control. C, apoptosis induction was assessed by oligonucleosomal fragmentation after a 72-hour incubation with cercosporamide (0.156–10 μmol/L). Data are shown relative to DMSO controls set at 1.0 ± SEM. D, apoptosis induction in HCT116 cells by cercosporamide was assessed ± the caspase inhibitor ZVAD (2.5 μmol/L). Data are shown relative to DMSO control set at 1.0 ± SEM.

Discussion

Though dispensable for normal organismal development (19), Mnk function and eIF4E phosphorylation may be essential for malignant transformation (8–10). Accordingly, Mnk may be an ideal target for cancer therapy. In the murine *Eμ-Myc* lymphoma model, constitutively activated Mnk promotes lymphomagenesis, whereas expression of dominant-negative Mnk suppresses lymphomagenesis and prolongs survival. Further, mutation of eIF4E serine 209 to alanine precludes Mnk-mediated eIF4E phosphorylation and also blocks lymphomagenesis (8). Likewise, engineered genetic disruption of eIF4E phosphorylation prevents tumor development in *PTEN*-null murine lymphoma and prostate cancer models (9, 10). Similarly, the efficiency with which eIF4E transforms cultured cells is dependent upon Mnk-mediated phosphorylation of eIF4E at serine 209 (17). Recent evidence has now shown that eIF4E phosphorylation is also commonly elevated in primary human cancer tissues (9, 23, 24) and predicts poorer survival in non–small-cell lung cancer and prostate cancer patients (9, 23, 25). Collectively, these data implicate Mnk-mediated eIF4E phosphorylation in malignant transformation and substantiate the notion that Mnk inhibition may be an attractive anticancer therapy.

We report here that the known antifungal agent, cercosporamide, is a potent, selective inhibitor, particularly of Mnk2. Cercosporamide demonstrated an *in vitro* IC_{50} of 11 nmol/L for Mnk2 and 116 nmol/L for Mnk1. Cercosporamide treatment rapidly and effectively blocked eIF4E phosphorylation in cultured cancer cells from multiple cell lineages, suppressing proliferation and soft agar colonization as well as inducing apoptosis. Oral administration of cercosporamide to xenograft-bearing mice also effectively inhibited eIF4E phosphorylation in xenografted tumor and mouse liver tissues as quickly as 30 minutes after administration and, with daily oral dosing of cercosporamide (20 mg/kg), significantly suppressed growth of subcutaneously implanted HCT116 human tumor xenografts. Finally, in experimental metastasis assays with the B16 mouse melanoma model, cercosporamide administration at 10 or 20 mg/kg significantly suppressed the outgrowth

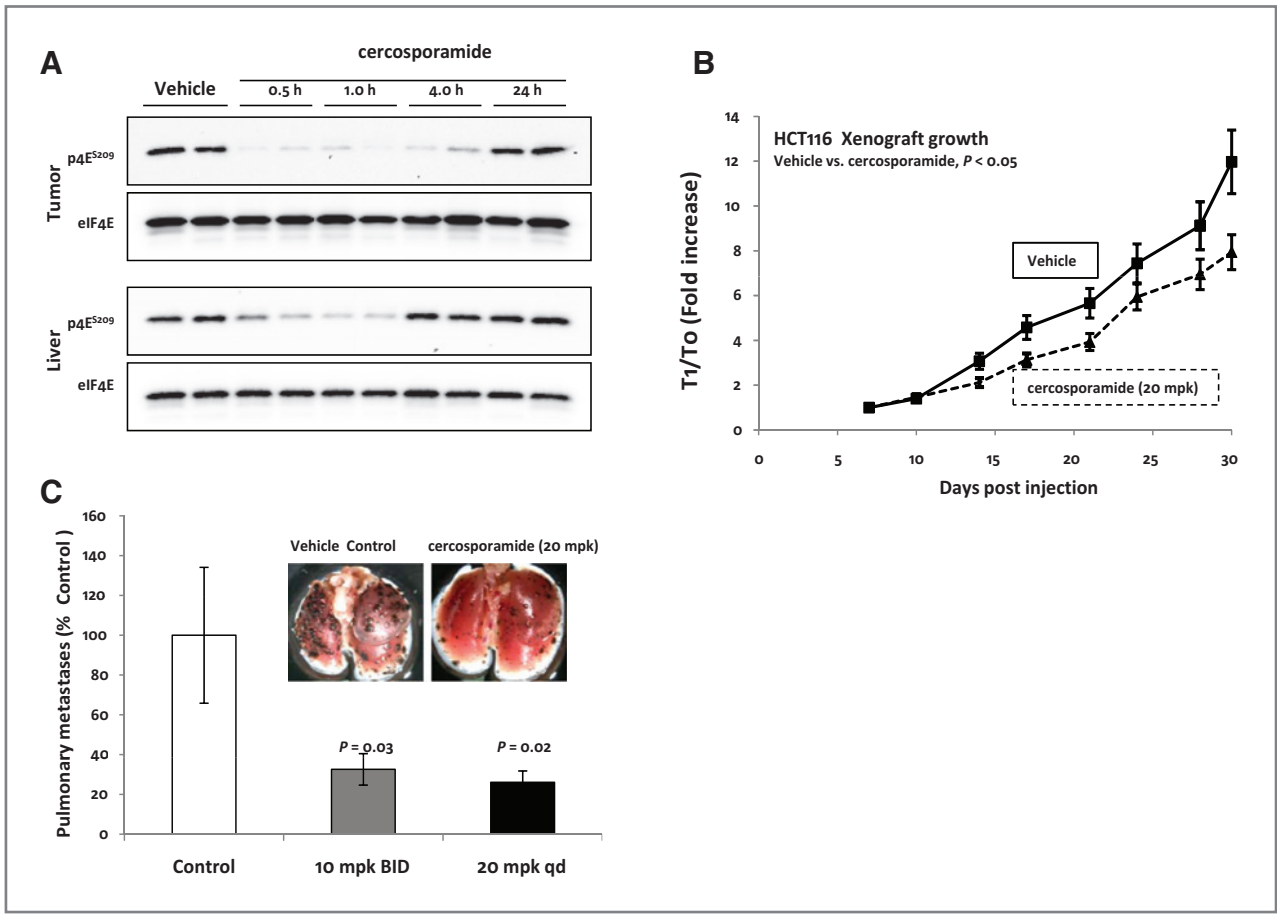

Figure 4. Cercosporamide blocks eIF4E serine 209 phosphorylation *in vivo,* reduces tumor growth, and suppresses B16 melanoma metastases. A, HCT116 xenograft-bearing nude mice were dosed once with cercosporamide p.o. by gavage (20 mg/kg). Xenograft tumor and mouse liver tissues were harvested at the indicated times postdose to evaluate eIF4E serine 209 phosphorylation by Western blotting. Companion blots were also run for total eIF4E protein. All blots were reprobed for β-actin to control for protein loading and transfer. B, HCT116 xenograft-bearing nude mice were dosed daily (20 mg/kg) for 30 days by gavage with cercosporamide. Tumors were measured twice weekly. Data shown represent tumor volumes at each measured time-point divided by initial tumor volume for each animal (T_1/T_0) ± SEM. Cercosporamide significantly suppressed HCT116 xenograft growth ($P < 0.05$, repeated measures analyses). Data are representative of 2 separate xenograft efficacy studies. C, nude mice were inoculated by tail vein injection with B16 melanoma cells. Starting 24 hours later, mice were treated 12 consecutive days p.o. by gavage with cercosporamide 10 mg/kg twice daily or 20 mg/kg. After 12 days, mice were killed to harvest lungs and count pigmented metastases. Data are shown as percent of vehicle treated controls ± SEM and represent 4 independent experiments. Inset- representative photomicrographs of lungs from mice treated with vehicle or cercosporamide (20 mg/kg).

of experimental pulmonary metastases without substantially altering mouse body weight.

Mnk can be activated as a downstream consequence of both ERK and p38MAPK signaling (7, 37). Mnk can interact directly with eIF4G and can, as a consequence of this association with the eIF4F complex, phosphorylate eIF4E at serine 209 (5, 6). This phosphorylation event has been associated with increased protein synthesis, cellular proliferation, survival, and malignant transformation in multiple experimental systems (17, 38–40). eIF4E phosphorylation has been the focus for these studies as eIF4E is the most extensively studied substrate of Mnk particularly with respect to malignancy. However, there are other Mnk substrates, including sprouty (41), cPLA2 (42) and hnRNPA1 (7, 43). How these proteins may be affected by Mnk in relation to malignancy is currently unclear and will be the subject of future experimentation.

The data provided in this manuscript reveal that cercosporamide is a potent Mnk inhibitor with selectivity for Mnk2. These data also show that cercosporamide is orally bioavailable, thus enabling pharmacologic inhibition of Mnk in experimental animal models of cancer. Indeed, cercosporamide treatment effectively inhibited phosphorylation of eIF4E *in vivo,* blocked xenograft tumor growth and suppressed the outgrowth of experimental pulmonary metastases. These data demonstrate the utility of this compound in probing Mnk function *in vitro* and *in vivo* and highlight the potential anticancer therapeutic utility of suppressing Mnk function. Moreover, exploring the activity of cercosporamide, as well as the inhibitors of translation initiation such as ribavirin (27), the 4E-ASO (25), or 4E-G1 (28), in a range of preclinical cancer models may ultimately elucidate which approach to targeting translation initiation might be most promising.

Disclosure of Potential Conflicts of Interest

B.W. Konicek, J.R. Stephens, A.M. McNulty, R.B. Peery, C.A. Dumstorf, M.S. Dowless, P.W. Iversen, S. Parsons, K.E. Ellis, D.J. McCann, J.M. Yingling, L.F. Stancato, and J.R. Graff: employment, Eli Lilly and Company. N. Sonenberg: consultant, Eli Lilly and Company. The other authors disclosed no potential conflicts of interest.

The costs of publication of this article were defrayed in part by the payment of page charges. This article must therefore be hereby marked *advertisement* in accordance with 18 U.S.C. Section 1734 solely to indicate this fact.

Received September 8, 2010; revised December 28, 2010; accepted January 2, 2011; published OnlineFirst January 13, 2011.

References

1. De Benedetti A, Graff JR. eIF4E expression and its role in malignancies and metastasis. Oncogene 2004;23:3189–99.
2. Sonenberg N, Hinnebusch AG. Regulation of translation initiation in eukaryotes: mechanisms and biological targets. Cell 2009;136:731–45.
3. Ruggero D, Sonenberg N. The AKT of translation control. Oncogene 2005;24:7426–34.
4. Fukunaga R, Hunter T. Mnk1, a new MAP kinase-activated protein kinase, isolated by a novel expression screening method for identifying protein kinase substrates. EMBO J 1997;16:1921–33.
5. Pyronnet S, Imataka H, Gingras AC, Fukunaga R, Hunter T, Sonenberg N. Human eukaryotic initiation factor 4G (eIF4G) recruits mnk1 to phosphorylate eIF4E. EMBO J 1999;18:270–79.
6. Waskiewicz A, Flynn A, Proud CG, Cooper J. Mitogen-activated protein kinases activate the serine/threonine kinases Mnk1 and Mnk2. EMBO J 1997;16:1909–20.
7. Buxade M, Parra-Palau JL, Proud CG. The Mnks: MAP kinase-interacting kinases (MAP kinase signal-interacting kinases). Front Biosci 2008;13:5359–74.
8. Wendel HG, Silva RL, Malina A, Mills JR, Zhu H, Ueda T. Dissecting eIF4E action in tumorigenesis. Genes & Dev 2007;21:3232–37.
9. Furic L, Rong L, Larsson O, Koumakpayi IH, Yoshida K, Brueschke A, et al. eIF4E phosphorylation promotes tumorigenesis and is associated with prostate cancer progression. Proc Natl Acad Sci U S A 2010;107:14134–39.
10. Ueda T, Sasaki M, Elia AL, Chio II, Hamada K, Fukunaga R, et al. Combined deficiency for MAP kinase-interacting kinase 1 and 2 (Mnk1 and Mnk2) delays tumor development. Proc Natl Acad Sci U S A 2010;107:13984–90.
11. Rousseau D, Kaspar R, Rosenwald I, Gehrke L, Sonenberg N. Translation initiation of ornithine decarboxylase and nucleocytoplasmic transport of cyclin D1 mRNA are increased in cells overexpressing eukaryotic initiation factor 4E. Proc Natl Acad Sci U S A 1996; 93:1065–70.
12. Graff J, Konicek B, Carter J, Marcusson E. Targeting the translation initiation factor 4E for cancer therapy. Cancer Res 2008;68:631–34.
13. Lazaris-Karatzas A, Montine KS, Sonenberg N. Malignant transformation by a eukaryotic initiation factor subunit that binds to mRNA cap. Nature 1990;345:544–47.
14. Graff JR, Zimmer SG. Translational control and metastatic progression: enhanced activity of the mRNA cap binding protein eIF-4E selectively enhances translation of metastasis-related mRNAs. Clin Exp Metastasis 2003;20:265–73.
15. Ruggero D, Montanaro L, Ma L, Xu W, Londei P, Cordon-Cardo C, Pandolfi PP. The translation factor eIF4E promotes tumor formation and cooperates with c-Myc in lymphomagenesis. Nat Med 2004;10:484–86.
16. Wendel HG, De Stanchina E, Fridman JS, Malina A, Ray S, Kogan S, et al. Survival signaling by AKT and eIF4E in oncogenesis and cancer therapy. Nature 2004;428:332–37.
17. Topisirovic I, Ruiz-Gutierrez M, Borden K. Phosphorylation of the eukaryotic translation initiation factor eIF4E contributes to its transformation and mRNA transport activities. Cancer Res 2004;64:8639–8642.
18. Phillips A, Blaydes JP. Mnk1 and eIF4E are downstream effectors of MEKs in the regulation of the nuclear export of HDM2 mRNA. Oncogene 2008;27:1645–49.
19. Ueda T, Watanabe-Fukunaga R, Fukuyama H, Nagata S, Fukunaga R. Mnk2 and Mnk1 are essential for constitutive and inducible phosphorylation of eukaryotic initiation factor 4E but not for cell growth or development. Mol Cell Biology 2004;24:6539–49.
20. Armengol G, Rojo F, Castellví J, Iglesias C, Cuatrecasas M, Pons B, Baselga J, et al. 4EBinding Protein 1: A Key Molecular "Funnel Factor" in Human Cancer with Clinical Implications. Cancer Res 2007; 67:7551–55.
21. Rojo F, Najera L, Lirola J, Jiménez J, Guzmán M, Sabadell MD, et al. 4E-binding protein 1, a cell signaling hallmark in breast cancer that correlates with pathologic grade and prognosis. Clin Cancer Res 2007;13:81–9.
22. Graff JR, Konicek BW, Lynch RL, Dumstorf CA, Dowless MS, McNulty AM, et al. eIF4E activation is commonly elevated in advanced human prostate cancers and significantly related to reduced patient survival. Cancer Res 2009;69:3866–73.
23. Yoshizawa A, Kukuoka J, Shimizu S, Shilo K, Franks TJ, Hewitt SM, et al. Overexpression of phospho-eIF4E is associated with survival through AKT pathway in non-small cell lung cancer. Clin Cancer Res 2010;16:240–8.
24. Fan S, Ramalingam SS, Kauh J, Xu Z, Khuri FR, Sun SY. Phosphorylated eukaryotic translation initiation factor (eIF4E) is elevated in human cancer tissues. Cancer Biology Ther 2009;8:1463–1469.
25. Graff JR, Konicek BW, Vincent TM, Lynch RL, Monteith D, Weir SN, et al. Therapeutic suppression of translation initiation factor eIF4E expression reduces tumor growth without toxicity. J Clin Invest 2007;117:2638–48.
26. Kentsis A, Topisirovic I, Culjkovic B, Shao L, Borden K. Ribavirin suppresses eIF4E-mediated oncogenic transformation by physical mimicry of the 7-methyl guanosine mRNA cap. Proc Natl Acad Sci U S A 2004;101:18105–10.
27. Assouline S, Culjkovic B, Cocolakis E, Rousseau C, Beslu N, Amri A, et al. Molecular targeting of the oncogene eIF4E in acute myeloid leukemia (AML): a proof-of-principle clinical trial with ribavirin. Blood 2009;114:257–60.
28. Moerke N, Aktas H, Chen H, Cantel S, Reibarkh MY, Fahmy A, et al. Small-molecule inhibition of the interaction between the translation initiation factors eIF4E and eIF4G. Cell 2007;128:257–67.
29. Graff JR, McNulty AM, Hanna KR, Konicek BW, Lynch RL, Bailey SN, et al. The protein kinase C beta-selective inhibitor, Enzastaurin (LY317615.HCl), suppresses signaling through the AKT pathway, induces apoptosis, and suppresses growth of human colon cancer and glioblastoma xenografts. Cancer Res 2005;65:7462–9.
30. Knauf U, Tschopp C, Gram H. Negative regulation of protein translation by mitogen-activated protein kinase-interacting kinases 1 and 2. Mol Cell Biol 2001;21:5500–11.
31. Bain J, Plater L, Elliott M, Shpiro N, Hastie CJ, McLauchlan H, et al. The selectivity of protein kinase inhibitors: a further update. Biochem J 2007;408:297–315.
32. Sugawara F, Strobel S, Strobel G. The structure and biological activity of cercosporamide from Cercospordium henningsii. J Org Chem 1991;56:909–10.
33. Cornejo MG, Boggon TJ, Mercher T. JAK3: a two-faced player in hematological disorders. Int J Biochem Cell Biol 2009;41:2376–9.
34. Sussman A, Huss K, Chio LC, Heidler S, Shaw M, Ma D, et al. Discovery of cercosporamide, a known antifungal natural product, as a selective Pkc1 kinase inhibitor through high-throughput screening. Eukaryotic Cell 2004;3:932–43.
35. Rinker-Schaeffer CW, Graff JR, DeBenedetti A, Zimmer SG, Rhoads RE. Decreasing the level of translation initiation factor 4E with antisense RNA causes reversal of ras-mediated transformation and

tumorigenesis of cloned rat embryo fibroblasts. Int J Cancer 1993;55:841–7.
36. Graff JR, Boghaert ER, DeBenedetti A, Tudor DM, Zimmer SG. Reduction of translation initiation factor 4E reduces tumor growth, invasion and metastasis of ras-transformed cloned rat embryo fibroblast. Int J Cancer 1995;60:255–63.
37. Pyronnet S. Phosphorylation of the cap-binding protein eIF4E by the MAPK-activated protein kinase Mnk1. Biochem Pharmacol 2000;60:1237–43.
38. Bianchini A, Loiarro M, Bielli P, Busà R, Paronetto MP, Loreni F, et al. Phosphorylation of eIF4E by MNKs supports protein synthesis, cell cycle progression and proliferation in prostate cancer cells. Carcinogenesis 2008;12:2279–88.
39. LaChance PE, Miron M, Raught B, Sonenberg N, Lasko P. Phosphorylation of eukaryotic translation initiation factor 4E is critical for growth. Mol Cell Biol 2002;22:1656–63.
40. Muta D, Makino K, Nakamura H, Yano S, Kudo M, Kuratsu JI. Inhibition of eIF4E phosphorylation reduces cell growth and proliferation in primary central nervous system lymphoma cells. [published online ahead of print May 25, 2010]J Neurooncol doi 10.1007/s1.
41. Dasilva J, Xu L, Kim HJ, Miller WT, Bar-Sagi D. Regulation of sprouty stability by Mnk1-dependent phosphorylation. Mol Cell Biol 2006;26:1898–1907.
42. Hefner Y, Borsch-Haubold AG, Murakami M, Wilde JI, Pasquet S, Schieltz D, et al. Serine 727 phosphorylation and activation of cytosolic phospholipase A2 by MNK1-related protein kinasesJ Biol Chem 2000;275:37542–51.
43. Buxade M, Parra JL, Rousseau S, Shpiro N, Marquez R, Morrice N, et al. The Mnks are novel components in the control of TNF alpha biosynthesis and phosphorylate and regulate hnRNP A1. Immunity 2005;23:177–89.